

# Base doping limits in heterostructure bipolar transistors

B. Jalali, R. N. Nottenburg, A. F. J. Levi, R. A. Hamm, M. B. Panish, D. Sivco, and A. Y. Cho

AT&T Bell Laboratories, Murray Hill, New Jersey 07974

(Received 16 November 1989; accepted for publication 14 February 1990)

Heterostructure bipolar transistors are used to experimentally determine band offsets in lattice-matched  $\text{In}_{0.53}\text{Ga}_{0.47}\text{As}$  devices. Valence-band offsets of  $\Delta E_V = 0.24$  eV for  $\text{Al}_{0.48}\text{In}_{0.52}\text{As}/\text{In}_{0.53}\text{Ga}_{0.47}\text{As}$  and  $\Delta E_V = 0.34$  eV for  $\text{InP}/\text{In}_{0.53}\text{Ga}_{0.47}\text{As}$  are measured. Because of band filling in the base, these values place important constraints on  $p$ -type doping levels and emitter injection efficiency in practical devices.

The base resistance  $R_B$  in a  $n$ - $p$ - $n$  bipolar transistor may be reduced by using high  $p$ -type impurity levels because majority-carrier mobility decreases sublinearly at high doping levels. The resultant reduction in circuit-charging time constant,  $R_B C$ , is important for high-speed electronics. In fact, base resistance is a critical issue in microwave bipolar transistors and was the motivator for the original heterostructure bipolar transistor (HBT) concept in which the base doping could be increased somewhat without decreasing current gain  $\beta$ .<sup>1</sup> Recent work has shown that growth of high quality layers of InGaAs lattice matched to InP with  $p$ -type doping  $> 10^{20} \text{ cm}^{-3}$  is possible.<sup>2</sup> These results, together with new insight into the physics of extreme nonequilibrium electron transport in heavily doped semiconductors, have fueled interest in  $n$ - $p$ - $n$  HBTs with base doping levels which were once thought to be impractical.<sup>3,4</sup> It is therefore relevant to ask what the maximum useful doping level in a HBT is.

As base doping is increased beyond  $10^{19} \text{ cm}^{-3}$ , one might intuitively expect an increase in minority-carrier scattering and a decrease in current gain  $\beta$ . However, previous work has shown that the total scattering rate (inelastic plus elastic) remains almost constant (it actually decreases slightly) for  $p > 5 \times 10^{19} \text{ cm}^{-3}$  and that base transport in thin-base HBTs should not limit  $\beta$ .<sup>3</sup> It turns out that for  $p > 10^{19} \text{ cm}^{-3}$ , the loss of carrier confinement is the critical issue. In a HBT the valence-band offset,  $\Delta E_V$ , between the wide-band-gap emitter and the narrow-band-gap base acts as a barrier to injection of holes into the  $N$ -type emitter. Thus the current gain  $\beta$  of an ideal transistor is limited by the back injection of holes.

In this letter, we have determined conduction- and valence-band offsets, energy gap, and hole Fermi energy in  $\text{Al}_{0.48}\text{In}_{0.52}\text{As}/\text{In}_{0.53}\text{Ga}_{0.47}\text{As}$  and  $\text{InP}/\text{In}_{0.53}\text{Ga}_{0.47}\text{As}$  HBTs by measuring the transistor characteristics in the forward and reverse active modes as a function of temperature  $T$ . In addition, we show that because of band filling in the base, there exists a trade-off between the need for low  $R_B$  and high  $\beta$ .

AllInAs/InGaAs devices were grown by conventional effusion cell molecular beam epitaxy (MBE) while InP/InGaAs transistors were grown by hydride source MBE (HSMBE) as outlined in Refs. 5 and 6. The collector consists of a 5000-Å-thick heavily doped  $n$ -InGaAs contact layer and a 3000-Å-thick InGaAs active region doped to  $n = 1 \times 10^{16} \text{ cm}^{-3}$ . The base region consists of an InGaAs active region of thickness  $Z_B$  doped to either  $p = 2 \times 10^{19}$ ,

$1 \times 10^{20}$ , or  $5 \times 10^{20} \text{ cm}^{-3}$ . Undoped spacer layers in the base with thicknesses in the range 25–100 Å were used depending on the growth temperature, Be concentration, and base thickness  $Z_B$ . The wide-band-gap emitter consists of a 2000-Å-thick AllInAs or InP layer doped to  $N = 1 \times 10^{18} \text{ cm}^{-3}$  and a 1000-Å-thick AllInAs or InP layer doped to  $N > 1 \times 10^{19} \text{ cm}^{-3}$ .

Figure 1(a) shows the energy band diagram of the HBT in forward active mode. The collector current is limited by electron thermionic emission over the abrupt conduction-band emitter-base barrier of energy  $\Delta E_C$ . In this situation the collector saturation current is given by the familiar Richardson expression

$$J_{\text{thermionic}} = A^* T^2 \exp(-q\Phi_{Bn}/k_B T), \quad (1)$$

where

$$q\Phi_{Bn} = E_{gb} + E_{F_h} + (\Delta E_C - qV_p). \quad (2)$$

In the above expressions,  $A^*$  is the effective Richardson constant,  $k_B$  is the Boltzmann constant,  $q$  is the electronic charge,  $E_{gb}$  is the band gap of the base,  $E_{F_h}$  is the Fermi energy of holes measured from the valence-band edge,  $\Delta E_C$  is the conduction-band discontinuity, and  $V_p$  is the diffusion potential developed in the base. For a base doping  $p = 2 \times 10^{19} \text{ cm}^{-3}$  and emitter doping  $N = 1 \times 10^{18} \text{ cm}^{-3}$ ,  $V_p = 30$  mV. The value of  $\Delta E_C$  may be obtained from Eq. (2) if  $E_{gb}$  and  $E_{F_h}$  are known. From the activation energy of the collector saturation current in the temperature range  $T = 160$ – $390$  K, we obtain a potential barrier  $\Phi_{Bn} = 1.25$  eV for an AllInAs/InGaAs HBT with  $p = 2 \times 10^{19} \text{ cm}^{-3}$ . It now remains to determine  $E_{gb} + E_{F_h}$ .

In the inverse active mode, shown in Fig. 1(b), collector current is given by electron diffusion across the InGaAs base. In the diffusion process, the temperature coefficient of the saturation current is determined by activation of minority-carrier density. Therefore, measuring the activation energy of collector current in inverse mode yields  $E_{gb} + E_{F_h}$ . Values for InGaAs doped to  $p = 2 \times 10^{19} \text{ cm}^{-3}$  and  $p = 1 \times 10^{20} \text{ cm}^{-3}$  are listed in Table I. The conduction-band discontinuity  $\Delta E_C$  and valence-band discontinuity  $\Delta E_V = \Delta E_g - \Delta E_C$  ( $\Delta E_g$  is the difference between the emitter and base band gaps) are also listed in Table I. The band gap of the emitter  $E_g$  was determined from photoluminescence measurements. The values  $\Delta E_V = 0.24$  eV for AllInAs/InGaAs and  $\Delta E_V = 0.34$  eV for InP/InGaAs are in good agreement with previous work.<sup>7–10</sup>

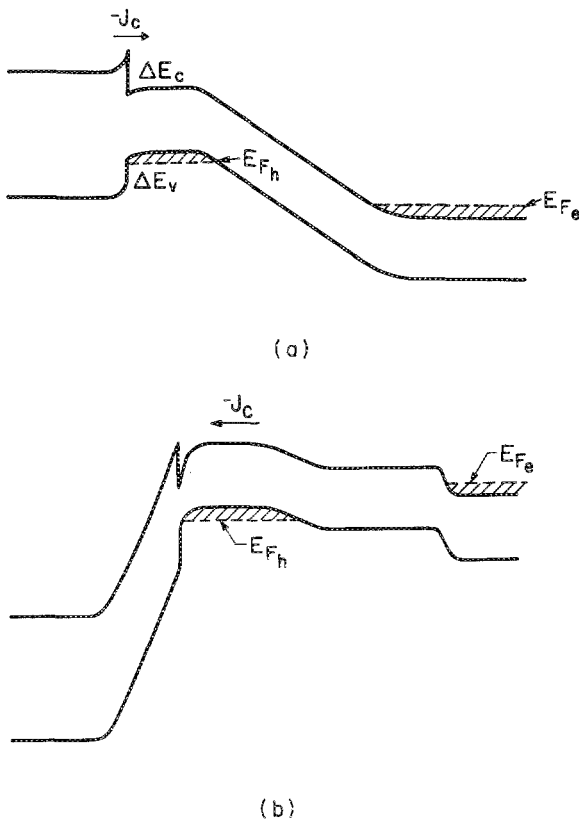


FIG. 1. Energy-band diagram for a HBT in (a) forward active and (b) inverse active modes showing conduction-band offset  $\Delta E_c$ , valence-band offset  $\Delta E_v$ , and hole Fermi energy  $E_{F_h}$ .

The band-gap and hole Fermi energy vary with base doping concentration. Although there is no available data for the amount of band-gap narrowing in heavily doped InGaAs, we can estimate its magnitude from our experimental data and calculation of hole Fermi energy. In our analysis, we assume that the valence bands of InGaAs are isotropic around  $k = 0$  and treat nonparabolicity in the light hole band using the  $\mathbf{k}\cdot\mathbf{p}$  approach.<sup>11</sup> Hole concentration is then given by<sup>12</sup>

$$p = 2 \left[ k_B (T/2\pi\hbar^2) \right]^{3/2} \left\{ m_{hh}^{3/2} F_{1/2}(W) + m_{lh}^{3/2} \times [F_{1/2}(W) - 15\gamma k_B (T/4E_g) F_{3/2}(W)] \right\}, \quad (3)$$

where  $m_{hh}$  and  $m_{lh}$  are  $k = 0$  heavy hole and light hole masses, respectively, and  $F_j(W)$  is the Fermi-Dirac integral for the reduced energy  $W = (E - E_F)/k_B T$ . The factor  $\gamma = -(1 + E_g/2\Delta_{so}) / (1 - E_g/2\chi)^2$  is the nonparaboli-

TABLE I. Measured energy-band parameters for the  $\text{Al}_{0.48}\text{In}_{0.52}\text{As}/\text{In}_{0.53}\text{Ga}_{0.47}\text{As}$  and  $\text{InP}/\text{In}_{0.53}\text{Ga}_{0.47}\text{As}$  heterostructures.

	$\text{Al}_{0.48}\text{In}_{0.52}\text{As}/\text{In}_{0.53}\text{Ga}_{0.47}\text{As}$ (eV)	$\text{InP}/\text{In}_{0.53}\text{Ga}_{0.47}\text{As}$ (eV)
$E_{cb}$	0.76 eV	0.76 eV
$E_{vc}$	1.48	1.35
$\Delta E_c$	0.48	0.25
$\Delta E_v$	0.24	0.34

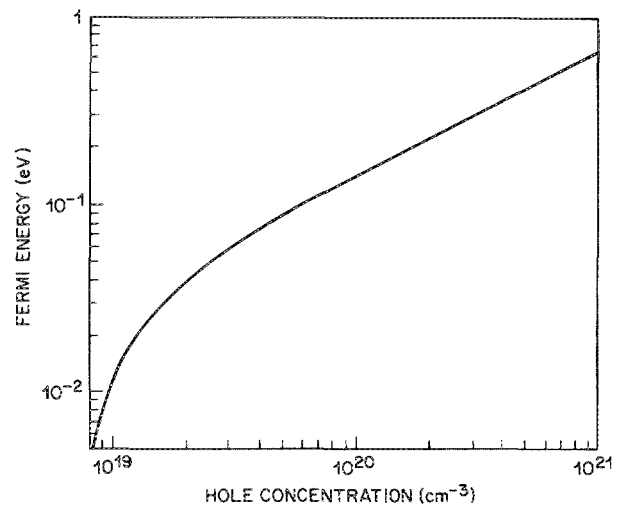


FIG. 2. Calculated hole Fermi energy  $E_{F_h}$  as function of majority-carrier concentration in the base.

city parameter where  $\Delta_{so}$  is the spin-orbit splitting, and  $\chi$  is the momentum matrix element corresponding to interaction between different bands and can be estimated from the band-edge effective mass of the light hole band ( $m_{lh} = 0.051m_0$ , Ref. 13).

Figure 2 shows the calculated room-temperature hole Fermi energy as a function of carrier concentration in the range  $10^{18} \text{ cm}^{-3} < p < 10^{21} \text{ cm}^{-3}$ . The effective density of states in the valence bands of  $\text{In}_{0.53}\text{Ga}_{0.47}\text{As}$  is  $\sim 7 \times 10^{18} \text{ cm}^{-3}$ . For hole concentrations above this value, Fermi energy moves inside the valence band. At  $p = 2 \times 10^{19} \text{ cm}^{-3}$  and  $p = 1 \times 10^{20} \text{ cm}^{-3}$  we obtain  $E_{F_h} = 40$  and 150 meV, respectively. From Fig. 2 and Table I it is obvious that the large increase in  $E_{F_h}$  (approximately scaling as  $p^{2/3}$ ) dominates over band-gap narrowing. For  $E_{F_h} = 150$  meV the effective valence-band barrier of an  $\text{AlInAs}/\text{InGaAs}$  device is reduced to 90 meV at room temperature ( $T = 300 \text{ K}$ ) and 190 meV for an  $\text{InP}/\text{InGaAs}$  device. It is clear from the results in Table I that the  $\text{InP}/\text{In}_{0.53}\text{Ga}_{0.47}\text{As}$  heterojunction has a greater valence-band offset than  $\text{Al}_{0.48}\text{In}_{0.52}\text{As}/\text{In}_{0.53}\text{Ga}_{0.47}\text{As}$ . As a consequence, an  $\text{InP}/\text{In}_{0.53}\text{Ga}_{0.47}\text{As}$  HBT is better able to confine carriers to a heavily doped  $p$ -type base region thereby minimizing back injection of holes into the  $N$ -type emitter. It should be noted that, in calculating the Fermi energy at very high carrier concentrations, one needs to include terms higher than fourth order in the energy dispersion relation, and thus the  $\mathbf{k}\cdot\mathbf{p}$  approximation becomes less accurate. However, since the underlying physics, namely, the restriction imposed on electron population by the exclusion principle, remains the same, the phase space filling will still be severe.

The practical limits to  $p$ -type doping level have been explored by measuring the static common emitter current gain  $\beta$  of a number of samples with varying base thickness  $Z_B$  and  $p$ -type doping level. Measured room-temperature ( $T = 300 \text{ K}$ ) values of  $\beta$  are plotted as a function of  $Z_B$  for  $p = 1 \times 10^{20} \text{ cm}^{-3}$  in Fig. 3. As may be seen, current gain rapidly decreases from  $\beta = 45$  at  $Z_B = 500 \text{ \AA}$  to  $\beta = 10$  at

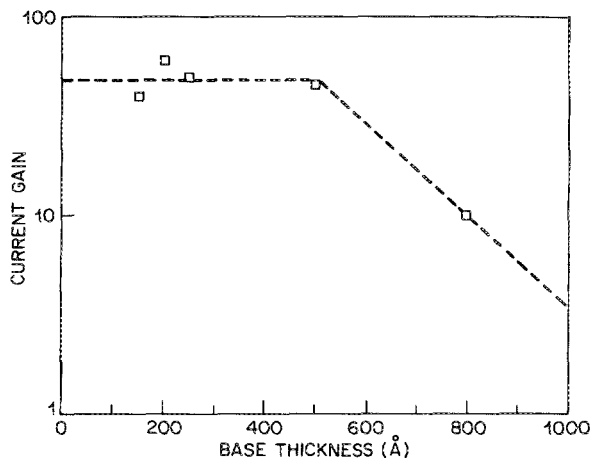


FIG. 3. Dependence of common emitter current gain  $\beta$  on base thickness  $Z_B$  for InP/InGaAs HBTs with base doping  $p = 1 \times 10^{20} \text{ cm}^{-3}$ .

$Z_B = 800 \text{ \AA}$ . The decrease in  $\beta$  with increasing base thickness  $Z_B$  is expected and is due to the increased probability of electron scattering in a thicker base and the subsequent increase in base current. However, for  $Z_B < 400 \text{ \AA}$  current gain is constant at  $\beta \approx 50$ . The current gain is now limited by back injection of holes into the  $N$ -type emitter rather than the probability of conduction-band electron scattering in the base. The importance of this result is that for  $p = 1 \times 10^{20} \text{ cm}^{-3}$ ,  $\beta$  is limited to a modest value by majority-carrier confinement. Thus an InP/In<sub>0.53</sub>Ga<sub>0.47</sub>As  $N$ - $p$ - $n$  HBT optimized for maximum  $\beta$  and minimum  $R_B$  with  $p = 1 \times 10^{20} \text{ cm}^{-3}$  has a base width of  $Z_B \approx 500 \text{ \AA}$  resulting in  $R_B \approx 350 \Omega \square^{-1}$ . The measured static transfer characteristics for a device with  $Z_B \approx 200 \text{ \AA}$  and  $p = 1 \times 10^{20} \text{ cm}^{-3}$  are shown in Fig. 4. As expected, the measured ideality factor for the base current is unity, and the current gain is limited by the back injection of holes. By increasing the base doping to  $p = 5 \times 10^{20} \text{ cm}^{-3}$  base resistance can be reduced to  $R_B \approx 125 \Omega \square^{-1}$  for  $Z_B = 500 \text{ \AA}$ . Although the increase in  $p$  is not expected to increase electron scattering in the base,<sup>3</sup> reduction in  $p$ -type carrier confinement due to the increase in Fermi energy  $E_{F_p}$  results in a dramatic reduction in the experimentally measured current gain from  $\beta = 45$  for  $p = 1 \times 10^{20} \text{ cm}^{-3}$  to  $\beta = 12$  for  $p = 5 \times 10^{20} \text{ cm}^{-3}$ . Thus, there are practical limits governing emitter injection efficiency beyond which it becomes difficult to exploit the advantages of high base doping in HBTs.

In conclusion, we have experimentally determined band offsets in In<sub>0.53</sub>Ga<sub>0.47</sub>As HBTs using low-temperature electrical and photoluminescence measurements. Our results indicate a valence-band offset  $\Delta E_V = 0.25 \text{ eV}$  for Al<sub>0.48</sub>In<sub>0.52</sub>As/In<sub>0.53</sub>Ga<sub>0.47</sub>As and  $\Delta E_V = 0.35 \text{ eV}$  for InP/In<sub>0.53</sub>Ga<sub>0.47</sub>As. Thus, InP/In<sub>0.53</sub>Ga<sub>0.47</sub>As HBTs with

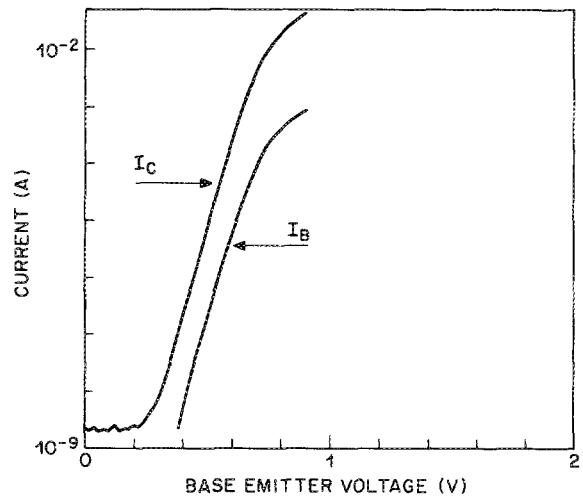


FIG. 4. Transfer characteristics for an InP/InGaAs HBT with base thickness  $Z_B = 200 \text{ \AA}$  and base doping  $p = 1 \times 10^{20} \text{ cm}^{-3}$ .

a heavily doped  $p$ -type base have better emitter injection efficiency. However, the need for low base resistance while maintaining useful values of current gain in a transistor ( $\beta \approx 50$ ) limits base doping levels to around  $(1-5) \times 10^{20} \text{ cm}^{-3}$ . Exploitation of the benefits of even higher doping levels requires improved carrier confinement which might be possible by, for example, increasing the indium content in the base.

The authors thank Y. K. Chen for useful discussions and acknowledge D. A. Humphrey and T. Fullowan for their help with device fabrication.

<sup>1</sup>H. Kromer, Proc. IEEE 70, 13 (1983).

<sup>2</sup>R. A. Hamm, M. B. Panish, R. N. Nottenburg, Y. K. Chen, and D. A. Humphrey, Appl. Phys. Lett. 54, 2586 (1989).

<sup>3</sup>A. F. J. Levi, Electron. Lett. 24, 1273 (1988).

<sup>4</sup>R. N. Nottenburg, Y. K. Chen, M. B. Panish, R. Hamm, and D. A. Humphrey, IEEE Electron Dev. Lett. EDL-9, 524 (1988); Y. K. Chen, R. N. Nottenburg, M. B. Panish, R. A. Hamm, and D. A. Humphrey, *ibid.* EDL-10, 267 (1989).

<sup>5</sup>Morton B. Panish and Henryk Temkin, Annu. Rev. Mater. Sci. 9, 209 (1989).

<sup>6</sup>B. Jalali, R. N. Nottenburg, Y. K. Chen, A. F. J. Levi, D. Sivco, A. Y. Cho, and D. A. Humphrey, Appl. Phys. Lett. 54, 2333 (1989).

<sup>7</sup>R. People, K. W. Wecht, K. Alavi, and A. Y. Cho, Appl. Phys. Lett. 43, 118 (1983).

<sup>8</sup>D. V. Lang, M. B. Panish, F. Capasso, J. Allam, R. A. Hamm, and A. M. Sargent, Appl. Phys. Lett. 50, 736 (1987).

<sup>9</sup>P. E. Brunemeier, D. G. Deppe, and N. Holonyak, Jr., Appl. Phys. Lett. 46, 755 (1985).

<sup>10</sup>D. Ortel, D. Bimberg, and R. K. Bauer, Appl. Phys. Lett. 55, 140 (1989).

<sup>11</sup>E. O. Kane, J. Phys. Chem. Solids 1, 249 (1957).

<sup>12</sup>J. S. Blakemore, J. Appl. Phys. 53, 123 (1982).

<sup>13</sup>C. Hermann and T. P. Pearsall, Appl. Phys. Lett. 8, 450 (1980).